

# Spectral and FTIR Analysis of Ho<sup>3+</sup> ions doped Zinc Lithium Calcium Potassiumniobate Phosphate Glasses

Pankaj Deedwaniya and S.L. Meena

Ceramic Laboratory, Department of physics, Jai Narain Vyas University, Jodhpur 342001 (Raj.) India

## Abstract

Glass of the system: (45-x)P<sub>2</sub>O<sub>5</sub>:10ZnO:10Li<sub>2</sub>O:10CaO:10K<sub>2</sub>O:15Nb<sub>2</sub>O<sub>5</sub>:xHo<sub>2</sub>O<sub>3</sub> (where x=1, 1.5, 2 mol %) have been prepared by melt-quenching method. The amorphous nature of the prepared glass samples was confirmed by X-ray diffraction. Optical absorption, Excitation, fluorescence and FTIR spectra were recorded at room temperature for all glass samples. Judd-Ofelt intensity parameters  $\Omega_{\lambda}$  ( $\lambda=2, 4$  and  $6$ ) are evaluated from the intensities of various absorption bands of optical absorption spectra. Using these intensity parameters various radiative properties like spontaneous emission probability (A), branching ratio ( $\beta$ ), radiative life time ( $\tau_R$ ) and stimulated emission cross-section ( $\sigma_p$ ) of various emission lines have been evaluated.

**Keywords:** ZLCPNP Glasses, Optical Properties, FTIR Spectroscopy, Judd-Ofelt Theory.

Date of Submission: 02-11-2022

Date of Acceptance: 13-11-2022

## I. Introduction

Glasses doped with rare earth ions have attracted a great deal of attention because of their applications in laser fusion, optical fibers, sensors, infrared detectors, marine optical communications, up-conversion lasers, optical data storage and high density memory storage devices [1–5]. Among different glasses, phosphate glasses have unique properties. They have high transparency, high thermal stability, lower phonon energy, high refractive index and high density [6–11]. Addition of network modifier (NMF) Li<sub>2</sub>O to the phosphate glasses improves both electrical and mechanical properties of such glasses [12, 13]. The addition of ZnO increases both the tendency of glass formation, refractive index while decreases the optical energy band gap [14]. Ho<sup>3+</sup> doped glasses are very important because of the possibility of their application in optoelectronic and optic device fields, such as lasers, fiber optics and solar cells [15–21].

The present work reports on the preparation and characterization of rare earth doped heavy metal oxide (HMO) glass systems for lasing materials. We have studied on the Optical absorption, Excitation, fluorescence and FTIR spectra of Ho<sup>3+</sup> doped zinc lithium calcium potassiumniobate phosphate glasses. The intensities of the transitions for the rare earth ions have been estimated successfully using the Judd-Ofelt theory, The laser parameters such as radiative probabilities (A), branching ratio ( $\beta$ ), radiative life time ( $\tau_R$ ) and stimulated emission cross section ( $\sigma_p$ ) are evaluated using J.O. intensity parameters ( $\Omega_{\lambda}$ ,  $\lambda=2, 4$  and  $6$ ).

## II. Experimental Techniques

### Preparation of glasses

The following Ho<sup>3+</sup> doped phosphate glass samples (45-x)P<sub>2</sub>O<sub>5</sub>:10ZnO:10Li<sub>2</sub>O:10CaO:10K<sub>2</sub>O:15Nb<sub>2</sub>O<sub>5</sub>:xHo<sub>2</sub>O<sub>3</sub> (where x=1, 1.5 and 2 mol%) have been prepared by melt-quenching method. Analytical reagent grade chemical used in the present study consist of P<sub>2</sub>O<sub>5</sub>, ZnO, Li<sub>2</sub>O, CaO, K<sub>2</sub>O, Nb<sub>2</sub>O<sub>5</sub> and Ho<sub>2</sub>O<sub>3</sub>. They were thoroughly mixed by using an agate pestle mortar. then melted at 1075<sup>0</sup>C by an electrical muffle furnace for 2h., After complete melting, the melts were quickly poured in to a preheated stainless steel mould and annealed at temperature of 250<sup>0</sup>C for 2h to remove thermal strains and stresses. Every time fine powder of cerium oxide was used for polishing the samples. The glass samples so prepared were of good optical quality and were transparent. The chemical compositions of the glasses with the name of samples are summarized in **Table 1**.

**Table 1.**

Chemical composition of the glasses

Sample	Glass composition (mol %)
ZLCPNP(UD)	45P <sub>2</sub> O <sub>5</sub> :10ZnO:10Li <sub>2</sub> O:10CaO:10K <sub>2</sub> O:15Nb <sub>2</sub> O <sub>5</sub>
ZLCPNP (HO1)	44P <sub>2</sub> O <sub>5</sub> :10ZnO:10Li <sub>2</sub> O:10CaO:10K <sub>2</sub> O:15Nb <sub>2</sub> O <sub>5</sub> :1 Ho <sub>2</sub> O <sub>3</sub>
ZLCPNP(HO1.5)	43.5P <sub>2</sub> O <sub>5</sub> :10ZnO:10Li <sub>2</sub> O:10CaO:10K <sub>2</sub> O:15Nb <sub>2</sub> O <sub>5</sub> :1.5Ho <sub>2</sub> O <sub>3</sub>

ZLCPNP(HO2) 43P<sub>2</sub>O<sub>5</sub>:10ZnO:10Li<sub>2</sub>O:10CaO:10K<sub>2</sub>O:15Nb<sub>2</sub>O<sub>5</sub>:2H<sub>2</sub>O<sub>3</sub>ZLCPNP (UD) -Represents undoped Zinc Lithium Calcium Potassium niobate phosphate glass specimens  
ZLCPNP(HO)-Represents  $\text{Ho}^{3+}$  doped Zinc Lithium Calcium Potassium niobate phosphate glass specimens

### III. Theory

#### 3.1 Oscillator Strength

The intensity of spectral lines are expressed in terms of oscillator strengths using the relation [22].

$$f_{\text{expt.}} = 4.318 \times 10^{-9} \int \epsilon(\nu) d\nu \quad (1)$$

where,  $\epsilon(\nu)$  is molar absorption coefficient at a given energy  $\nu$  ( $\text{cm}^{-1}$ ), to be evaluated from Beer–Lambert law. Under Gaussian Approximation, using Beer–Lambert law, the observed oscillator strengths of the absorption bands have been experimentally calculated [23], using the modified relation:

$$P_m = 4.6 \times 10^{-9} \times \frac{1}{cl} \log \frac{I_0}{I} \times \Delta\nu_{1/2} \quad (2)$$

where  $c$  is the molar concentration of the absorbing ion per unit volume,  $l$  is the optical path length,  $\log I_0/I$  is optical density and  $\Delta\nu_{1/2}$  is half band width.

#### 3.2. Judd-Ofelt Intensity Parameters

According to Judd[24] and Ofelt[25] theory, independently derived expression for the oscillator strength of the induced forced electric dipole transitions between an initial  $J$  manifold  $|4f^N(S, L) J\rangle$  level and the terminal  $J'$  manifold  $|4f^N(S', L') J'\rangle$  is given by:

$$\frac{8\pi^2 m c \bar{\nu}}{3h(2J+1)n} \frac{1}{n} \left[ \frac{(n^2+2)^2}{9} \right] \times S(J, J') \quad \text{Where, the} \quad (3)$$

line strength  $S(J, J')$  is given by the equation

$$S(J, J') = e^2 \sum_{\lambda} \Omega_{\lambda} \langle 4f^N(S, L) J \| U^{(\lambda)} \| 4f^N(S', L') J' \rangle^2 \quad (4)$$

$\lambda = 2, 4, 6$

In the above equation  $m$  is the mass of an electron,  $c$  is the velocity of light,  $\nu$  is the wave number of the transition,  $h$  is Planck's constant,  $n$  is the refractive index,  $J$  and  $J'$  are the total angular momentum of the initial and final level respectively,  $\Omega_{\lambda}$  ( $\lambda = 2, 4$  and  $6$ ) are known as Judd-Ofelt intensity.

#### 3.3 Radiative Properties

The  $\Omega_{\lambda}$  parameters obtained using the absorption spectral results have been used to predict radiative properties such as spontaneous emission probability ( $A$ ) and radiative life time ( $\tau_R$ ), and laser parameters like fluorescence branching ratio ( $\beta_R$ ) and stimulated emission cross section ( $\sigma_p$ ).

The spontaneous emission probability from initial manifold  $|4f^N(S', L') J'\rangle$  to a final manifold  $|4f^N(S, L) J\rangle$  is given by:

$$A[(S', L') J'; (S, L) J] = \frac{64 \pi^2 \bar{\nu}^3}{3h(2J'+1)} \left[ \frac{n(n^2+2)^2}{9} \right] \times S(J', J) \quad (5)$$

$$\text{Where, } S(J', J) = e^2 [\Omega_2 \| U^{(2)} \|^2 + \Omega_4 \| U^{(4)} \|^2 + \Omega_6 \| U^{(6)} \|^2]$$

The fluorescence branching ratio for the transitions originating from a specific initial manifold  $|4f^N(S', L') J'\rangle$  to a final manifold  $|4f^N(S, L) J\rangle$  is given by

$$\beta[(S', L') J'; (S, L) J] = \frac{A[(S', L) J]}{\sum_{(S', L') J'} A[(S', L') J']} \quad (6)$$

$S, L, J$

where, the sum is over all terminal manifolds.

The radiative life time is given by

$$\tau_{\text{rad}} = \sum A[(S', L') J'; (S, L) J] = A_{\text{Total}}^{-1} \quad (7)$$

S L J

where, the sum is over all possible terminal manifolds. The stimulated emission cross-section for a transition from an initial manifold  $|4f^N(S', L') J' \rangle$  to a final manifold  $|4f^N(S, L) J \rangle$  is expressed as

$$\sigma_p(\lambda_p) = \left[ \frac{\lambda_p^4}{8\pi c n^2 \Delta\lambda_{\text{eff}}} \right] \times A[(S', L') J'; (\bar{S}, \bar{L}) \bar{J}] \quad (8)$$

where,  $\lambda_p$  the peak fluorescence wavelength of the emission band and  $\Delta\lambda_{\text{eff}}$  is the effective fluorescence line width.

### 3.4 Nephelauxetic Ratio ( $\beta'$ ) and Bonding Parameter ( $b^{1/2}$ )

The nature of the R-O bond is known by the Nephelauxetic Ratio ( $\beta'$ ) and Bonding Parameters ( $b^{1/2}$ ), which are computed by using following formulae [26, 27]. The Nephelauxetic Ratio is given by

$$\beta' = \frac{\nu_g}{\nu_a} \quad (9)$$

where,  $\nu_a$  and  $\nu_g$  refer to the energies of the corresponding transition in the glass and free ion, respectively. The value of bonding parameter ( $b^{1/2}$ ) is given by

$$b^{1/2} = \left[ \frac{1-\beta'}{2} \right]^{1/2} \quad (10)$$

## IV. Result and Discussion

### 4.1 XRD Measurement

Figure 1 presents the XRD pattern of the sample contain  $-\text{P}_2\text{O}_5$  which is show no sharp Bragg's peak, but only a broad diffuse hump around low angle region. This is the clear indication of amorphous nature within the resolution limit of XRD instrument.

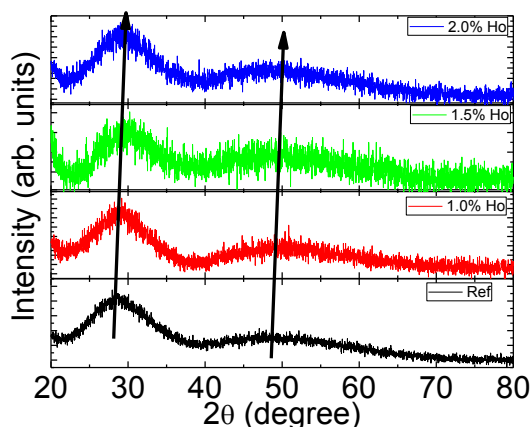


Fig. 1 X-ray diffraction pattern of ZLCPNP (HO) Glasses.

### 4.2 FTIR Transmission spectra

The FTIR spectrum of ZLCPNP(HO 01) glass is in the wave number range  $500-4000\text{cm}^{-1}$  is presented in Fig.2 and the possible mechanism bands are tabulated in Table 2.

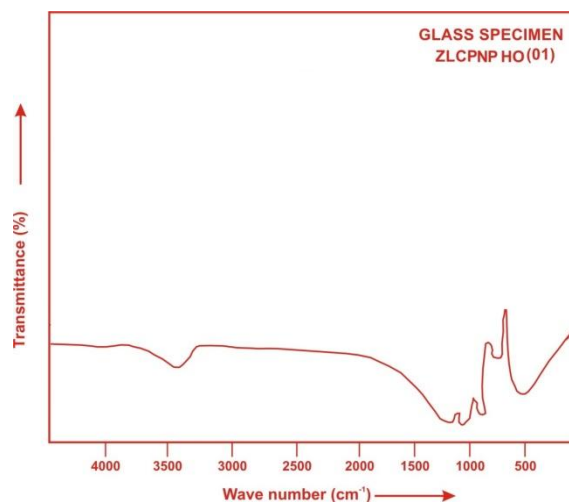


Fig. (2) FTIR spectrum of ZLCPNP HO (01) glass.

The band observed at  $525\text{ cm}^{-1}$  is attributed to the P-O-P bending vibrations [20]. The observed band around  $750\text{ cm}^{-1}$  is due to the P-O-P symmetric stretching vibrations while the occurrence of band around  $926\text{ cm}^{-1}$  is assigned to the P-O-P asymmetric stretching vibrations [21, 22]. The Asymmetric stretching modes of  $(\text{PO}_3)^{2-}$  groups is observed around  $1110\text{ cm}^{-1}$  [23]. The Asymmetric stretching vibration of P=O and O-P-O bonds is observed around  $1235\text{ cm}^{-1}$  [24]. The observed band around  $3425\text{ cm}^{-1}$  is attributed to symmetric stretching vibrations of the O-H bonds [25].

Table 2. Assignment of infrared transmission bands of (ZLCPNP HO 01) glass.

Peak position ( $\text{cm}^{-1}$ )	Band Assignment
~ 525	Bending vibration of P-O-P bands
~ 750	Symmetric stretching vibration of P-O-P bonds
~ 926	Asymmetric stretching vibration of P-O-P bonds
~ 1110	Asymmetric stretching modes of $(\text{PO}_3)^{2-}$ groups
~ 1235	Asymmetric Stretching Vibration of P=O and O-P-O bonds
~ 3425	Symmetric stretching of the O-H bonds

### 4.3 Absorption Spectrum

The absorption spectra of  $\text{Ho}^{3+}$  doped ZLCPNP glass specimens have been presented in Figure 3 in terms of optical density versus wavelength. Twelve absorption bands have been observed from the ground state  $^5\text{I}_8$  to excited states  $^5\text{I}_5$ ,  $^5\text{I}_4$ ,  $^5\text{F}_5$ ,  $^5\text{F}_4$ ,  $^5\text{F}_3$ ,  $^3\text{K}_8$ ,  $^5\text{G}_6$ ,  $(^5\text{G}, ^3\text{G})_5$ ,  $^5\text{G}_4$ ,  $^5\text{G}_2$ ,  $^5\text{G}_3$ , and  $^3\text{F}_4$  for  $\text{Ho}^{3+}$  doped ZLCPNP glasses.

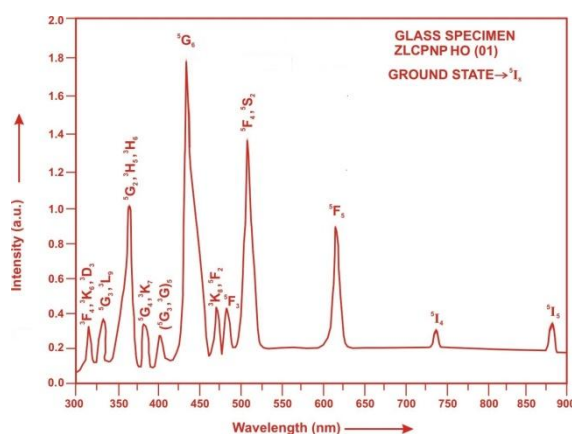


Fig. (3) Absorption spectrum of ZLCPNP HO (01) glass.

The experimental and calculated oscillator strength for  $\text{Ho}^{3+}$  ions in ZLCPNP glasses are given in **Table 3**.

**Table 3:** Measured and calculated oscillator strength ( $P_m \times 10^{+6}$ ) of  $\text{Ho}^{3+}$  ions in ZLCPNP glasses.

Energy level from $^5\text{I}_8$	Glass ZLCPNP(HO01)		Glass ZLCPNP(HO1.5)		Glass ZLCPNP(HO02)	
	$P_{\text{exp}}$	$P_{\text{cal}}$	$P_{\text{exp}}$	$P_{\text{cal}}$	$P_{\text{exp}}$	$P_{\text{cal}}$
$^5\text{I}_5$	0.48	0.25	0.43	0.24	0.39	0.23
$^3\text{I}_4$	0.06	0.02	0.05	0.02	0.04	0.02
$^5\text{F}_5$	3.68	2.84	3.43	2.72	3.38	2.69
$^5\text{F}_4$	4.72	4.39	4.64	4.25	4.59	4.19
$^5\text{F}_3$	1.62	2.44	1.55	2.37	1.48	2.34
$^3\text{K}_8$	1.50	2.00	1.41	1.93	1.37	1.89
$^5\text{G}_6$	25.78	25.75	24.26	24.26	23.13	23.15
$(^3\text{G}, ^3\text{G})_5$	3.95	1.73	3.76	1.63	3.72	1.61
$^5\text{G}_4$	0.04	0.62	0.03	0.59	0.02	0.58
$^5\text{G}_2$	5.65	5.48	5.60	5.19	5.53	4.98
$^5\text{G}_3$	1.48	1.41	1.43	1.36	1.38	1.33
$^3\text{F}_4$	1.36	4.25	1.32	4.02	1.28	3.97
r.m.s. deviation	1.1335		1.0787		1.0797	

Computed values of  $F_2$ , Lande' parameter ( $\xi_{4f}$ ), Nephelauxetic ratio ( $\beta'$ ) and bonding parameter ( $b^{1/2}$ ) for  $\text{Ho}^{3+}$  ions in ZLCPNP glass specimen are given in Table 4.

**Table 4:**  $F_2, \xi_{4f}, \beta'$  and  $b^{1/2}$  parameters for Holmium doped glass specimen.

Glass Specimen	$F_2$	$\xi_{4f}$	$\beta'$	$b^{1/2}$
$\text{Ho}^{3+}$	358.82	1258.16	0.9337	0.1821

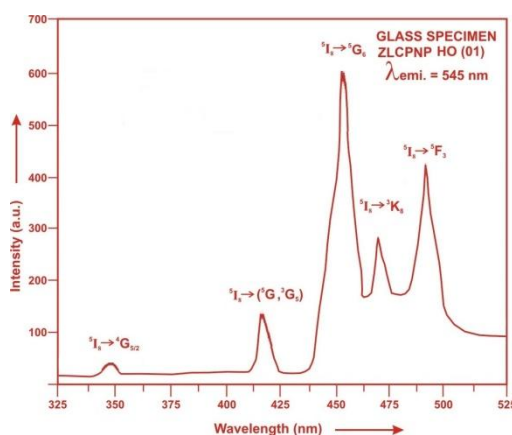
In the Zinc Lithium Calcium Potassium niobate Phosphate glasses (ZLCPNP)  $\Omega_2, \Omega_4$  and  $\Omega_6$  parameters decrease with the increase of x from 1 to 2 mol%. The order of magnitude of Judd-Ofelt intensity parameters is  $\Omega_2 > \Omega_6 > \Omega_4$  for all the glass specimens. The spectroscopic quality factor ( $\Omega_4/\Omega_6$ ) related with the rigidity of the glass system has been found to lie between 0.598 and 0.617 in the present glasses. The values of Judd-Ofelt intensity parameters are given in Table 5.

**Table 5:** Judd-Ofelt intensity parameters for  $\text{Ho}^{3+}$  doped ZLCPNP glass specimens.

Glass Specimen	$\Omega_2(\text{pm}^2)$	$\Omega_4(\text{pm}^2)$	$\Omega_6(\text{pm}^2)$	$\Omega_4/\Omega_6$
ZLCPNP (HO01)	6.356	1.392	2.256	0.6170
ZLCPNP (HO1.5)	5.982	1.304	2.188	0.5960
ZLCPNP HO02)	5.657	1.290	2.158	0.5978

#### 4.4 Excitation Spectrum

The Excitation spectrum of ZLCPNP (HO 01) glass has been presented in Figure 4 in terms of Excitation Intensity versus wavelength. The excitation spectrum was recorded in the spectral region 325–525 nm fluorescence at 545 nm having different excitation band centered at 349, 419, 450, 473 and 486 nm are attributed to the  $^5\text{G}_3, (^3\text{G}, ^3\text{G})_5, ^5\text{G}_6, ^3\text{K}_8$  and  $^2\text{F}_3$  transitions, respectively. The highest absorption level is  $^5\text{G}_6$  and is at 450 nm. So this is to be chosen for excitation wavelength.

**Fig. (4)** Excitation spectrum of ZLCPNP HO (01) glass.

#### 4.5 Fluorescence Spectrum

The fluorescence spectrum of Ho<sup>3+</sup> doped in zinc lithium calcium potassium niobate phosphate glass is shown in Figure 5. There are five broad bands observed in the fluorescence spectrum of Ho<sup>3+</sup> doped zinc lithium calcium potassium niobate phosphate glass. The wavelengths of these bands along with their assignments are given in Table 6. The peak with maximum emission intensity appears at 501 nm and corresponds to the (<sup>3</sup>F<sub>4</sub>→<sup>5</sup>I<sub>8</sub>) transition.

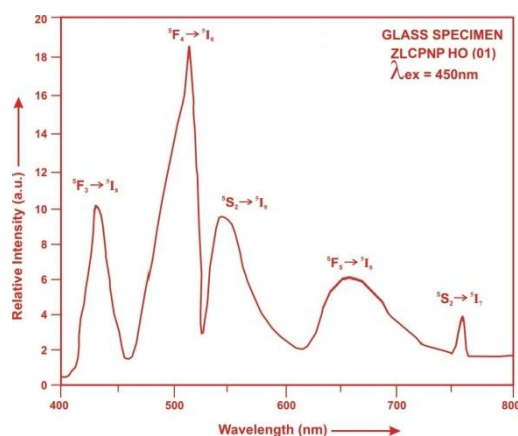


Fig. (5). Fluorescence spectrum of ZLCPNP HO (01) glass.

**Table 6: Emission peak wave lengths ( $\lambda_p$ ), radiative transition probability ( $A_{rad}$ ), branching ratio ( $\beta$ ), stimulated emission cross-section ( $\sigma_p$ ) and radiative life time ( $\tau_R$ ) for various transitions in Ho<sup>3+</sup> doped ZLCPNP glasses.**

Transition	ZLCPNP(HO 01)					ZLCPNP(HO 1.5)				ZLCPNP (HO 02)			
	$\lambda_{max}$ (nm)	$A_{rad}(s^{-1})$	$\beta$	$\sigma_p$ (10 <sup>-20</sup> cm <sup>2</sup> )	$\tau_R(\mu s)$	$A_{rad}(s^{-1})$	$\beta$	$\sigma_p$ (10 <sup>-20</sup> cm <sup>2</sup> )	$\tau_R(\mu s)$	$A_{rad}(s^{-1})$	$\beta$	$\sigma_p(10^{-20} \text{ cm}^2)$	$\tau_R(10^{-20} \text{ cm}^2)$
<sup>3</sup> F <sub>3</sub> → <sup>5</sup> I <sub>8</sub>	435	4138.30	0.2646	0.530	6395.12	4024.36	0.2657	0.506	6602.25	3977.11	0.2656	0.489	6679.20
<sup>3</sup> F <sub>4</sub> → <sup>5</sup> I <sub>8</sub>	501	6582.29	0.4209	1.181		6363.06	0.4201	1.121		6290.86	0.4202	1.082	
<sup>5</sup> S <sub>2</sub> → <sup>5</sup> I <sub>8</sub>	555	1727.64	0.1105	0.403		1679.82	0.1109	0.385		1660.10	0.1109	0.374	
<sup>3</sup> F <sub>3</sub> → <sup>5</sup> I <sub>8</sub>	652	1877.33	0.1201	0.718		1804.75	0.1192	0.681		1784.39	0.1192	0.658	
<sup>5</sup> S <sub>2</sub> → <sup>5</sup> I <sub>7</sub>	761	1311.35	0.0839	0.970		1274.36	0.0841	0.933		1259.40	0.0841	0.904	

#### V. Conclusion

In the present study, the glass samples of composition (45-x)P<sub>2</sub>O<sub>5</sub>:10ZnO:10Li<sub>2</sub>O:10CaO:10K<sub>2</sub>O:15Nb<sub>2</sub>O<sub>5</sub>:xHo<sub>2</sub>O<sub>3</sub>. (where x = 1, 1.5 and 2 mol %) have been prepared by melt-quenching method. The value of stimulated emission cross-section ( $\sigma_p$ ) is found to be maximum for the transition (<sup>5</sup>F<sub>4</sub>→<sup>5</sup>I<sub>8</sub>) for glass ZLCPNP(HO 01), suggesting that glass ZLCPNP (HO 01) is better compared to the other two glass systems ZLCPNP (HO1.5) and ZLCPNP(HO02). The large stimulated emission cross section in bismuth borate glasses suggests the possibility of utilizing these systems as laser materials. The FTIR of glasses revealed the presence of characteristic bonding vibrations of different functional groups.

#### References

- Monisha, M., Nancy, A., Souza, D., Jegde, V., Prabhu, N.S. and Sayyed, M.I. (2020). Dy<sup>3+</sup>-doped SiO<sub>2</sub>-B<sub>2</sub>O<sub>3</sub>-Al<sub>2</sub>O<sub>3</sub>-NaF-ZnF<sub>2</sub> glasses: An exploration of optical and gamma radiation shielding features, *Current Applied Physics* 20(11), 1207-1210.
- Prabhu, N. S., Hegde, V., Sayyed, M.I., Agar, O., Kamath, S. D. (2019). Investigations on structural and radiation shielding properties of Er<sup>3+</sup> doped zinc bismuth borate glasses, *Materials chemistry and physics*, 230, 267-276.
- Meena, S.L. (2019). Spectral and Thermal properties of Sm<sup>3+</sup> doped zinc lithium Tungsten Antimony Germanate Glasses, *Journal of Pure and Industrial physics*. 9(12), 82-90.
- Dousti, M.R., Poirier, G.Y., de Camargo, A.S.S. (2020). Tungsten Sodium Phosphate glasses doped with trivalent rare earth ions (Eu<sup>3+</sup>, Tb<sup>3+</sup>, Nd<sup>3+</sup>, Er<sup>3+</sup>) for visible and near infrared applications, *Journal of Non-Crystalline Solids* 530, 119838.
- Kaur, R. and Khanna, A. (2020). Photoluminescence and thermal properties of trivalent ion-doped lanthanum tellurite anti-glass composite samples, *Journal of Luminescences*, 117375.
- Kaur, M., Singh, L., Singh, A. and Thakur, V. (2014). Synthesis and characterization of Dy<sup>3+</sup> doped phosphate Glasses, *International Journal of Education and Applied Research* 4. Int. J. of Educ. and app. research, 4(2), 47-48.
- Damodaraiah, S., Prasad, V. R., Vijaya Lakshmi, R.P. and Ratnakaram, Y.C. (2019). Luminescence behaviour and phonon sideband analysis of europium doped Bi<sub>2</sub>O<sub>3</sub> based phosphate glasses for red emitting device applications, *Optical Materials* 92, 352-358.
- Hongisto, M., Vebar, A., Giovanna, N., Danto, S., Veronique and Petit, L. (2020). Transparent Yb<sup>3+</sup>-doped phosphate glass ceramics, *Ceramics International* 46(16), 26317-26325.
- Li, H., Yi, J., Qin, Z., Sun, Z., Xu, Y., Wang, C., Zhao, F., Hao, Y. and Xiaofeng L. (2019). Structures, Thermal expansion, chemical stability and crystallization behavior of phosphate based glasses by influence of rare earth, *Journal of Non-Crystalline Solids* 522, 119602.

- [10]. LiyuHao, Manting Pei, Tie Yang, Chengguo Ming(2020).Double sensitivity temperature sensor based on excitation intensity ratio of Eu<sup>3+</sup> doped phosphate glass ceramic, *Optik* 204,164188.
- [11]. Chowdhury,S.,Mandal, P.,andGhosh, S.(2019). Structural properties of Er<sup>3+</sup> doped lead zinc phosphate glasses, *Mat. Sci. and Eng.*,240,116-120.
- [12]. Devi, R.and Jayasankar, C. K.(1995).Optical properties of Nd<sup>3+</sup> ions in lithium borate glasses, *Materials chemistry and physics*, 42,106-119.
- [13]. Anjaiah, J. and Laxmikanth, C.(2015). Optical Properties of Neodymium Ion Doped Lithium Borate Glasses, 5,173 -183.
- [14]. Noorazlan, A. M., Kamari, H. M.,Zulkefly, S. S.andMohamad, D.W. (2013).Effect of erbium nanoparticles on optical properties of zincborotellurite glass system, *J.Nanomater*, 1–8
- [15]. Ravi Prakash, M., Neelima, G.,Kummara, V.K., Ravic, N.,DwarakaViswanath, C.S., SubbaRao, T.andMahaboobJilani, S.(2019). Holmium doped bismuth-germanate glasses for green lighting applications: A spectroscopic study. *Opt. Mater.*, 94, 436–443.
- [16]. Devaraja, C., JagadeeshaGowda, G.V.,Eraiah, B.,Keshavamurthy, K.(2021). Optical properties of bismuth tellurite glasses doped with holmium oxide. *Ceram. Int.*, 47, 7602–7607.
- [17]. Pan, Y., Bai, X., Feng, J., Huang, L., Li, G.,Chen, Y.(2022). Influences of holmium substitution on the phase structure and piezoelectric properties of BiFeO<sub>3</sub>-BaTiO<sub>3</sub>-based ceramics. *J. Alloys Compd.*, 918, 165582.
- [18]. Tsotetsi, D., Dhlamini, M. and Mbule, P.(2022). Sol-gel synthesis and characterization of Ho<sup>3+</sup> doped TiO<sub>2</sub> nanoparticles: Evaluation of absorption efficiency and electrical conductivity for possible application in perovskite solar cells. *Opt. Mater.* 2022, 130, 112569.
- [19]. Zhang, Y., Xia, L., Li, C., Ding, J., Li, J., Zhou, X.(2021). Enhanced 2.7 μm mid-infrared emission in Er<sup>3+</sup>/Ho<sup>3+</sup> co-doped tellurite glass. *Opt Laser Technol.*138,106913.
- [20]. Bentouila , O.,Aiadi,K.E., Rehouma, F.,Poulain, M.andBenhbirech, F.(2019).Thermal stability and spectroscopic study of Ho<sup>3+</sup>/Yb<sup>3+</sup> co-doped fluorophosphates glasses, *Journal of King Saud University – Science*,31,628-634.
- [21]. A. S Alqarni, R.Hussin, S.N.Alamri, S.K. Ghoshal(2020).Tailored structures and dielectric traits of holmium ion-doped zinc-sulpho-boro-phosphate glass ceramics,*Ceremics International* 46(3),3282-3291.
- [22]. Gorller-Walrand, C. and Binnemans, K. (1988). Spectral Intensities of f-f Transition. In: Gshneidner Jr., K.A. and Eyring,L., Eds.,*Handbook on the Physics and Chemistry of Rare Earths*, Vol. 25, Chap. 167, North-Holland, Amsterdam, 101-264.
- [23]. Sharma, Y.K., Surana, S.S.L. and Singh, R.K. (2009) Spectroscopic Investigations and Luminescence Spectra of Sm<sup>3+</sup> Doped SodaLime Silicate Glasses. *Journal of Rare Earths*, 27, 773-780.
- [24]. Judd, B.R. (1962). Optical Absorption Intensities of Rare Earth Ions. *Physical Review*, 127, 750-761.
- [25]. Ofelt, G.S. (1962). Intensities of Crystal Spectra of Rare Earth Ions. *The Journal of Chemical Physics*, 37, 511.
- [26]. Sinha, S.P. (1983).Systematics and properties of lanthanides, Reidel, Dordrecht.1-8.
- [27]. Krupke, W.F. (1974).IEEE J.Quantum Electron QE, 10,450.

Pankaj Deedwaniya, et. al. "Spectral and FTIR Analysis of Ho<sup>3+</sup> ions doped Zinc Lithium Calcium Potassiumniobate Phosphate Glasses." *International Journal of Engineering Science Invention (IJESI)*, Vol. 11(11), 2022, PP 01-07. Journal DOI- 10.35629/6734